# Gene disruption of p27$^{\text{Kip1}}$ allows cell proliferation in the postnatal and adult organ of Corti

HUBERT LÖWENHEIM*†, DAVID N. FURNESS‡, JONATHAN KIL§¶, CHRISTOPH ZINN‖, KARINA GÜLTIG*, MATTHEW L. FERO**, DEANNA FROST§, ANTHONY W. GUMMER‖, JAMES M. ROBERTS**, EDWIN W. RUBEL§, CAROLE M. HACKNEY‡, AND HANS-PETER ZENNER*

*Department of Otolaryngology, ‖Section of Physiological Acoustics and Communication, University of Tübingen, Silcherstrasse 5, 72076 Tübingen, Germany; ‡Department of Communication and Neuroscience, Keele University, Keele, Staffordshire ST5 5BG, United Kingdom; §Virginia Merrill Bloedel Hearing Research Center and Department of Otolaryngology-Head and Neck Surgery, University of Washington, Seattle, WA 98195; and **Department of Basic Sciences, Fred Hutchinson Cancer Research Center, 1124 Columbia Street, Seattle, WA 98104

**ABSTRACT** Hearing loss is most often the result of hair-cell degeneration due to genetic abnormalities or ototoxic and traumatic insults. In the postembryonic and adult mammalian auditory sensory epithelium, the organ of Corti, no hair-cell regeneration has ever been observed. However, nonmammalian hair-cell epithelia are capable of regenerating sensory hair cells as a consequence of nonsensory supporting-cell proliferation. The supporting cells of the organ of Corti are highly specialized, terminally differentiated cell types that apparently are incapable of proliferation. At the molecular level terminally differentiated cells have been shown to express high levels of cell-cycle inhibitors, in particular, cyclin-dependent kinase inhibitors [Parker, S. B., *et al.* (1995) *Science* **267**, 1024–1027], which are thought to be responsible for preventing these cells from reentering the cell cycle. Here we report that the cyclin-dependent kinase inhibitor p27$^{\text{Kip1}}$ is selectively expressed in the supporting-cell population of the organ of Corti. Effects of p27$^{\text{Kip1}}$-gene disruption include ongoing cell proliferation in postnatal and adult mouse organ of Corti at time points well after mitosis normally has ceased during embryonic development. This suggests that release from p27$^{\text{Kip1}}$-induced cell-cycle arrest is sufficient to allow supporting-cell proliferation to occur. This finding may provide an important pathway for inducing hair-cell regeneration in the mammalian hearing organ.

Sensory hair-cell loss is the major cause of permanent hearing loss. In mammals, including humans, hair cells do not regenerate spontaneously after loss caused by genetic or environmental factors. However, other vertebrate classes have retained the capacity to regenerate sensory hair cells (1–4). In birds, for example, the major early event in this hair-cell regeneration process is proliferation of supporting cells in the sensory epithelium (5, 6). Considerable progress has been made recently in understanding how supporting-cell proliferation is induced in the otherwise quiescent supporting-cell populations of the avian auditory epithelia and, to some extent, in the mammalian vestibular epithelia (7–9). These findings suggest that it might be possible to determine mechanisms that lead to stimulation of hair-cell regeneration in the bird auditory epithelium and to apply them to the seemingly similar postmitotic (10, 11) auditory epithelium of mammals, including humans (12). However, the mammalian auditory sensory epithelium, the organ of Corti, thus far has shown no ability to regenerate hair cells, and it has not proved possible to isolate the relevant factors or to produce the appropriate conditions to provoke supporting-cell proliferation in the organ of Corti (13–15).

The absence of any proliferative capacity in the organ of Corti may indicate that the supporting-cell population has attained a terminally differentiated state. By definition, terminal differentiation (16–19) comprises two interdependent and normally irreversible phenomena: permanent withdrawal from the cell cycle and phenotypic differentiation. In contrast, the supporting-cell population of the avian auditory epithelium is quiescent and has retained its capacity to proliferate in response to hair-cell loss. Therefore, this investigation has been directed at the potential role of cell-cycle inhibition in the supporting-cell population of the organ of Corti. Inhibitors of cell-cycle progression include the cyclin-dependent kinase inhibitors (CKIs), which function in both cell-cycle arrest and differentiation in other cell types. They exert these functions by binding to and inactivating cyclin–cyclin-dependent kinase (CDK) complexes. In particular, the CKIs of the Cip/Kip-family (p21$^{\text{Cip1}}$, p27$^{\text{Kip1}}$, and p57$^{\text{Kip2}}$) have been implicated in bringing about cell-cycle exit during development and in maintaining cells in a terminally differentiated state, demonstrating a cell-selective expression pattern in various organs (20–25). In this study, we evaluate the expression pattern and function of p27$^{\text{Kip1}}$ in the organ of Corti. We demonstrate that disruption of the p27$^{\text{Kip1}}$-gene in a knock-out mouse model promotes cell division in the postnatal and adult mouse organ of Corti well after terminal mitosis is normally completed at embryonic day 14 (11).

## METHODS

**Animals.** All mice used throughout this study were obtained from a breeding colony of mice with a p27$^{\text{Kip1}}$-gene disruption and maintained by coauthors (M.L.F. and J.M.R.) at the Fred Hutchinson Cancer Research Center (Seattle) (23). All mice were from a 129/Sv genetic background with no evident hearing abnormalities. The three different genotypes used are designated as p27+/+ for wild type, p27+/− for heterozygous, and p27−/− for homozygous null status for the p27$^{\text{Kip1}}$-gene.

**Immunohistochemistry.** Mice with a wild-type status (p27+/+) for the p27$^{\text{Kip1}}$-gene were used for immunolabeling of the p27$^{\text{Kip1}}$-protein in the organ of Corti. Mice with a homozygous disruption of the p27$^{\text{Kip1}}$-gene (p27−/−) were

---

used as negative controls. Mice were anesthetized with sodium pentobarbital (0.2 ml, i.p.) and decapitated, and the bullae were removed and opened. Cochleae were perfused with 4% paraformaldehyde in 0.15 M sodium PBS through the round window. Cochleae were immersion-fixed for an additional 30 min and rinsed in PBS. Tissues were paraffin-embedded and radially sectioned at 10-$\mu$m thickness. Adult tissues first were decalcified in 0.5 M EDTA for 3 weeks before sectioning. Sections were deparaffinized in xylene, rehydrated, and microwaved for 2–3 min in sodium citrate buffer (pH 6.0). Endogenous peroxidase activity was quenched in 90% methanol/0.3% $H_2O_2$ for 30 min. Tissues were blocked in 10% normal horse serum (NHS)/PBS for 30 min and incubated in primary antibody diluted 1:100 (p27$^{Kip1}$ mouse mAb, Neomarkers, Fremont, CA) for 1 h at room temperature (RT) or overnight at 4°C. A biotinylated secondary antibody diluted 1:200 was added followed by avidin–biotin complex (ABC) for 30 min each at RT (Vector Laboratories). Sections were stained in diaminobenzidine (DAB)/$H_2O_2$ for 8 min, coverslipped, and viewed by light microscopy with interference-contrast illumination.

**DNA Synthesis.** To determine the functional effects of p27$^{Kip1}$ gene disruption on cell proliferation in postnatal and adult mice cochleae of each genotype, BrdUrd was injected (30 mg/kg s.c. per single injection) into p27+/+ (wild type), p27+/− (heterozygote), and p27−/− (homozygote) mice. BrdUrd is a nucleotide analog that is incorporated into cells undergoing DNA synthesis. Injections were given to two different age groups of animals, postnatal and adult. In the postnatal group of p27+/+ ($n = 4$), p27+/− ($n = 6$), and p27−/− ($n = 4$) animals, injections (30 mg/kg s.c. each) were started on postnatal day 7 (1×), continued on P8 (2×), P9 (2×), and P10 (1×) for a total of six injections. A similar course of six injections (30 mg/kg s.c. each) was applied to adult (4-month-old) p27−/− ($n = 1$), p27+/− ($n = 2$), and p27+/+ ($n = 2$) animals.

Both the postnatal and the adult animals were sacrificed 1 day after the last injection (P11 for postnatal animals) by Nembutal sedation (i.p.) and transcardial perfusion of 10% formalin. The cochleae were dissected from the temporal bones and perfused with 4% paraformaldehyde in 0.15 M PBS through the round and oval windows. Cochleae were immersed in fixative for an additional 30 min. The cochlear bone and stria vascularis and tectorial membrane were dissected, and the organs of Corti were processed for BrdUrd immunocytochemistry. Tissues were rinsed in PBS and treated with 90% methanol/0.3% $H_2O_2$ for 20 min followed by 2 M HCl for 30 min. Tissues then were rinsed in PBS followed by incubation in a BrdUrd mouse IgG mAb (Becton Dickinson) diluted 1:50 in 2% NHS/0.05% Triton X-100/PBS for 1 h at RT. A biotinylated secondary antibody diluted 1:200 then was used followed by ABC for 30 min each at RT (Vector Laboratories). Whole mounts were stained in DAB/$H_2O_2$ for 5 min, rinsed, and coverslipped. A 1,000-$\mu$m length of the organ of Corti in the apical half of each cochlea was delimited by SCION IMAGING software using a light microscope coupled to a Macintosh computer via a CCD (charge-coupled device) camera. The sensory epithelium was identified under Nomarski optics. Counts of labeled cells were made along this length of the organ of Corti using a ×25 objective and a 10 × 10 reticule. Labeled cells were counted if they were located above the basilar membrane and within and between the inner hair-cell (IHC) region (medial limit) and the Hensen's-cell region (lateral limit). Labeled macrophages and phagocytes within the sensory epithelium and labeled cells within the inner and outer sulcus regions and below the basilar membrane were excluded. Both cochleae from each animal were examined. The number of cochleae analyzed in the postnatal group were p27+/+ ($n = 8$), p27+/− ($n = 12$), and p27−/− ($n = 8$) and

in the adult group were p27+/+ ($n = 4$), p27+/− ($n = 4$), and p27−/− ($n = 2$).

**Scanning Electron Microscopy (SEM).** Cochleae from postnatal (1-week-old) p27+/+ ($n = 4$), p27+/− ($n = 4$), and p27−/− ($n = 4$) and adult (4-month-old) p27+/+ ($n = 4$), p27+/− ($n = 4$), and p27−/− ($n = 4$) mice were fixed with 2.5% glutaraldehyde in 0.1 M sodium cacodylate buffer (pH 7.4) containing 2 mM calcium chloride by perfusion through the round window followed by immersion fixation for 2 h. Cochleae were postfixed for 1 h in 1% osmium tetroxide in the same buffer. Cochleae were washed in distilled water, placed in a saturated aqueous solution of sodium thiocarbohydrazide for 20 min, washed thoroughly in several changes of distilled water and immersed for 1 h in 1% osmium tetroxide. This treatment was repeated and the cochleae were dehydrated through an ethanolic series, critical-point-dried from $CO_2$, and mounted on scanning stubs using silver DAG electroconductive paint (Agar Scientific). They then were examined in a Hitachi S-4500 field emission electron microscope operated at an accelerating voltage of 5 kV.

**Transmission Electron Microscopy (TEM).** Cochleae from postnatal (1-week-old) p27+/+ ($n = 2$), p27+/− ($n = 2$), and p27−/− ($n = 2$) and adult (4-month-old) p27+/+ ($n = 4$), p27+/− ($n = 4$), and p27−/− ($n = 4$) mice were fixed with glutaraldehyde and osmium tetroxide as described for SEM. They then were dehydrated through an ethanolic series and vacuum-infiltrated with Spurr resin via a series of propylene oxide/resin mixtures over a 24-h period. The resin was polymerized at 60°C for 16 h, and ultrathin sections were cut in both the horizontal and radial planes. These were mounted on copper grids, stained using 2% ethanolic uranyl acetate and 2% lead citrate, and examined in a JEOL 100CX transmission electron microscope operated at 100 kV.

**Auditory Brainstem Response (ABR).** Additional 4-month-old, age-matched p27+/+ ($n = 2$), p27+/− ($n = 4$), and p27−/− ($n = 4$) mice were used to test ABR thresholds. Animals were anesthetized with ketamine (100 mg/kg) and xylazine (16 mg/kg) after premedication with atropine (2.5 mg/kg). Experiments were conducted in a sound-proof room. The active electrode (0.1-mm silver wire; Narishige, Tokyo) was placed s.c. near the external meatus of the ear to be assessed, a dural reference electrode was placed in a drilled hole 1 mm rostral to the bregma, and a ground electrode (Ag/AgCl$_2$ pellet) was placed in the back. A personal computer with a digital signal-processing (DSP) board operated by LABVIEW (National Instruments, Austin, TX) was used both for control of stimuli and signal recording. The sound-delivery system consisted of an acoustic coupler combining an AKG electrostatic speaker for sound presentation and a Brüel & Kjaer ¼-inch condenser microphone (4135; Brüel & Kjaer Naerum, Denmark) for sound-pressure measurement. The acoustic stimulus was a cosine$^2$-shaped tone pip of 1-ms duration and sound pressure up to 85 dB SPL (sound pressure level; relative 20 $\mu$Pa) presented at a rate of 10 Hz. Carrier frequencies of 4, 7, 10, 14, 16, 20, 30, 40, and 50 kHz were generated by using an SRS DS345 Function Generator. Brainstem responses were differentially amplified ×1,000, Bessel low-pass-filtered at 2 kHz, and averaged 200 times. Thresholds were determined visually in steps of 5 dB. Animal experiments were approved by the Committee for Animal Experiments of the Regional Council (Regierungspräsidium) of Tübingen.

## RESULTS

The expression of the p27$^{Kip1}$ antigen is confined to the supporting-cell population of the wild-type (p27+/+) mouse organ of Corti (Fig. 1). No staining was detected in the sensory hair cells. Labeled nuclei were present in all supporting-cell types, specifically the inner and outer pillar cells that form the tunnel of Corti and separate the IHCs from the outer hair cells
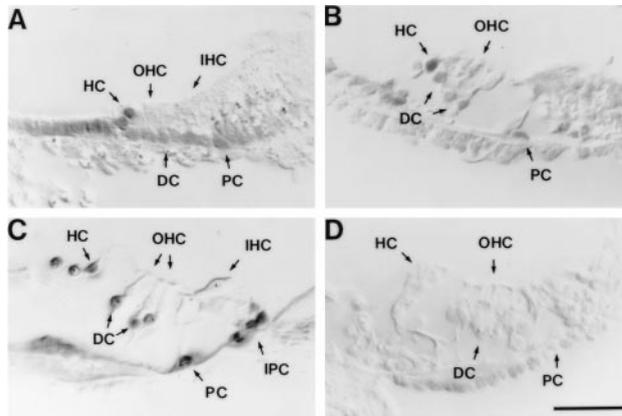
FIG. 1. Developmental expression of p27^Kip1 in the mouse organ of Corti revealed by immunocytochemistry in radial sections. The organ of Corti is composed of two sensory cell types arranged in one row of IHCs and three rows of OHCs. There are five different types of supporting cells whose nuclei lie below or adjacent to the hair-cell nuclei. These types include inner phalangeal cells (IPC), inner and outer pillar cells (PC), Deiters' cells (DC), and Hensen's cells (HC). Hair-cell and supporting-cell regions are indicated by arrows. Labeling with antibodies against p27^Kip1 shows that the protein is expressed only in the supporting-cell nuclei and not in the hair-cell nuclei. (*A*) Wild-type (p27+/+) mouse at postnatal day 0. (*B*) p27+/+ mouse at postnatal day 7; note the partially opened tunnel of Corti to the right of the outer PC. (*C*) p27+/+ adult mouse; note the fully opened tunnel of Corti. (*D*) The organ of Corti of the adult p27−/− animal shows no labeling; note the partially occluded tunnel of Corti. (Bar = 50 μm.)

(OHCs), the inner and outer phalangeal cells (Deiters' cells) that contact the bases and surround the apices of the IHCs and OHCs, respectively, and the Hensen's cells. Less intense labeling also was observed in nonsensory regions such as the inner and outer sulcus. This expression pattern is found at birth (Fig. 1*A*) and is maintained through later stages of development (Fig. 1 *B* and *C*). This is consistent with the hypothesis that p27^Kip1 may play a critical role in cell-cycle arrest and in maintaining the differentiated phenotype of the supporting-cell population in the developing and mature organ of Corti. No staining was detected in p27^Kip1-deficient (p27−/−) mice (Fig. 1*D*). Similar results have been obtained independently in embryonic and postnatal tissues (H. P. Chen and N. Segil, personal communication).

To determine the functional effects of gene disruption on proliferative behavior and differentiation in the organ of Corti, we investigated the morphology, proliferative capacity, and functional properties at postnatal and adult stages from p27^Kip1-deficient (p27−/−), heterozygous (p27+/−), and wild-type (p27+/+) mice. Mice from a 129/Sv genetic background with no evident hearing abnormalities were used throughout this study (23).

To determine whether proliferation occurs in postnatal and adult mice of each genotype, we injected BrdUrd to identify cells undergoing DNA synthesis in the organ of Corti of p27+/+, p27+/−, and p27−/− mice. No BrdUrd labeling was detected in the organ of Corti of p27+/+ control mice (Fig. 2*A*). However, BrdUrd-labeled cells were observed in all regions of the organ of Corti of p27−/− mice (Fig. 2*B*). Large numbers of BrdUrd-labeled cells were observed as doublets (Fig. 2*C*) and clusters in postnatal animals within both hair-cell and supporting-cell layers. In the adult mice the abundance of BrdUrd-labeled cells was reduced markedly, but single cells and doublets were still readily identified in both hair-cell and supporting-cell layers of the organ of Corti (Fig. 2*D*). No labeled cells were seen in the p27+/+ control mice of both postnatal and adult stages. Evidence of mitosis was also revealed at the ultrastructural level. Multiple cells within the
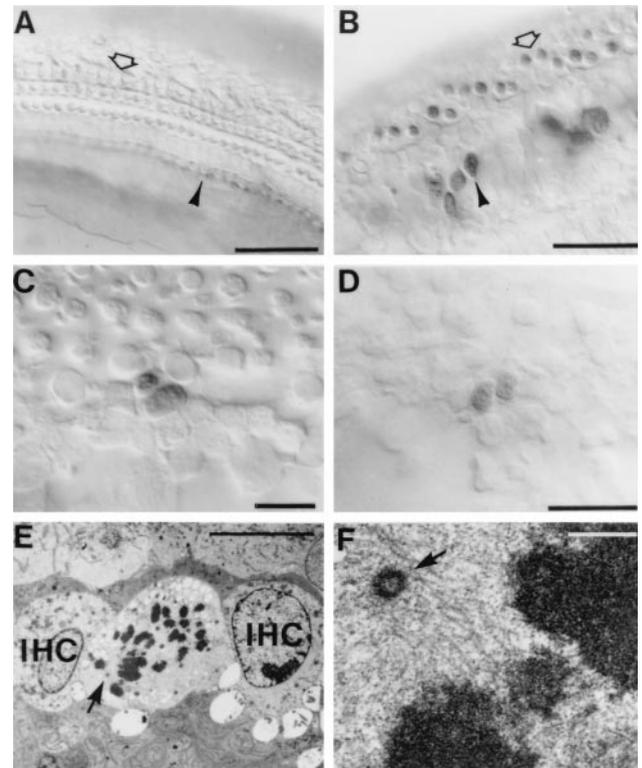


FIG. 2. Cell proliferation in the organ of Corti. (*A*) A whole-mount preparation of the p27+/+ organ of Corti at P11 after six BrdUrd injections between P7 and P10 to label proliferating cells. No BrdUrd-labeled cells are visible in the organ of Corti of p27+/+ control mice. (*B*) In p27−/− mice BrdUrd immunocytochemistry reveals labeled nuclei in the IHC (arrowhead) and OHC (open arrow) regions. (*C*) Higher magnification of a different region in the same animal shown in *B* demonstrating a BrdUrd-labeled doublet located at the luminal surface of the sensory epithelium between the pillar-cell region and the OHC region. (*D*) A whole-mount preparation of the p27−/− adult showing a BrdUrd-labeled doublet at the luminal surface of the sensory epithelium in the OHC region. (*E*) Transmission electron micrograph of a cell located between two IHCs containing condensed chromosomes in a P7 p27−/− pup. The arrow points to a region containing a centrosome and spindle microtubules. (*F*) The area indicated by the arrow in *E* is shown at a higher magnification revealing the centrosome (arrowhead) and associated microtubules. [Bars = 50 μm (*A* and *B*), 20 μm (*C* and *D*), 10 μm (*E*), 0.5 μm (*F*).]

sensory epithelium at various mitotic stages were identified by TEM in postnatal day 7 p27−/−mice (Fig. 2 *E* and *F*), clearly indicating that cell division was occurring in the sensory epithelium *in vivo*.

Specimens from postnatal p27−/− animals (*n* = 8 cochleae) injected with BrdUrd on postnatal days 7–10 averaged 80.3 ± 24.3 labeled cells (mean ± SD) over a 1,000-μm length (range of 58–108 labeled cells) in the apical half of the cochlea. In specimens from postnatal p27+/− (*n* = 12 cochleae) and p27+/+ (*n* = 8 cochleae) mice of identical age the counts revealed 2.8 ± 9.8 for p27+/− and 0.0 ± 0.0 for p27+/+, respectively. Statistical analysis revealed highly significant differences between p27−/− animals and the other two groups (*f* = 85.2; df = 2; *P* < 0.001). Statistics were determined by using ANOVA (STATVIEW 4.1). Only 1 of 12 cochleae from the postnatal group p27+/− cochlear specimens contained labeled cells (34 labeled cells/1,000-μm length of sensory epithelium), which were observed in the OHC region only. The 11 other p27+/− and all of the p27+/+ specimens contained no labeled cells in the sensory epithelium, which was consistent with the adult p27+/− and p27+/+ animals.

Specimens from adult p27−/− (*n* = 2 cochleae) mice averaged 8.5 ± 0.7 labeled cells (mean ± SD) over a 1,000-μm

length vs. specimens from p27 +/− ($n$ = 4 cochleae) (0.0 ± 0.0) and p27+/+ ($n$ = 4 cochleae) (0.0 ± 0.0). Statistical analysis revealed highly significant differences between p27−/− animals and the other two groups ($f$ = 809.2; df = 2; $P < 0.001$).

SEM observations of adult p27−/− mice showed significant alterations of the hair-cell and supporting-cell pattern compared with p27+/+ and p27+/− mice. Among the supporting-cell types, the inner pillar cells normally have rectangular apical surfaces and form a single row between the IHCs and OHCs (Fig. 3*A*). In the p27−/− mice these cells were not clearly discernible and there were additional cell surfaces of indeterminant cell type and irregular polygonal outlines visible in the same location (Fig. 3*B*). Up to three rows of cells could be detected between the row of IHCs and the first row of OHCs, with no clear distinction between inner and outer pillar-cell types (Fig. 3*B*). Examination by TEM revealed that another supporting-cell type, the Deiters' cells, also was altered. The normal organ of Corti has two to four Deiters'-cell phalangeal processes adjacent to an OHC of the second row (Fig. 3*C*). In the adult p27−/− mice there appeared to be up to six Deiters'-cell processes encircling each OHC (Fig. 3*D*). Tissue sections revealed that there was also an increase in the number of Deiters'-cell bodies relative to OHCs in p27−/− (Fig. 3 *E* and *F*), and SEM revealed an increased number of Hensen's-cell apices (data not shown). The tunnel of Corti was reduced markedly in cross-sectional area due to dysmorphic pillar cells (Fig. 3 *E* and *F*). Despite the distortion of the general cytoarchitecture, at the single-cell level pillar cells and Deiters' cells contained recognizable features of fully differentiated cells, such as large microtubular bundles (Fig. 3*F*). The adult p27+/− had a normal supporting-cell phenotype compared with the p27+/+, except for occasional additional pillar-cell heads (data not shown).

Examination of hair cells in the adult p27−/− showed that morphological abnormalities were present in some cells of the apical turn (Fig. 3 *B* and *F*), whereas in the basal turn, the OHCs were largely missing (Fig. 3*G*). No abnormalities were detected in hair cells of the adult p27+/− or p27+/+ organ of Corti. To determine whether the altered phenotype of the adult p27−/− resulted from abnormal early development or from continued proliferation in postnatal life, we investigated the organ of Corti at postnatal day 7. In 7-day-old animals a supporting-cell phenotype similar to that of the adult was already established (Fig. 3*H*), indicating that this abnormal phenotype was produced during embryonic or early postnatal development. At postnatal day 7, however, no hair-cell loss was apparent in the basal region, and, in fact, there appeared to be supernumerary rows of inner and outer hair cells at this location (Fig. 3*H*) when compared with p27+/+ controls (data not shown).

Consistent with these morphological findings, functional analysis by ABR showed substantially elevated thresholds for p27−/− mice as compared with p27+/− and p27+/+ animals across the entire frequency range examined (Fig. 4).

## DISCUSSION

These results demonstrate that p27$^{Kip1}$ plays an essential role in development of the organ of Corti as a cell-selective regulator of cell proliferation and contributes to the formation of the precise tissue architecture. Both effects are most apparent in the supporting-cell population, as might be expected from the fact that p27$^{Kip1}$ expression is confined to supporting cells (Fig. 1).

The effects of disrupting expression of p27$^{Kip1}$ on supporting-cell differentiation, as seen in the present study, may be a secondary consequence of the severe distortion of cytoarchitecture caused by the loss of proliferative inhibition in the sensory epithelium. Although p27$^{Kip1}$ has been demonstrated
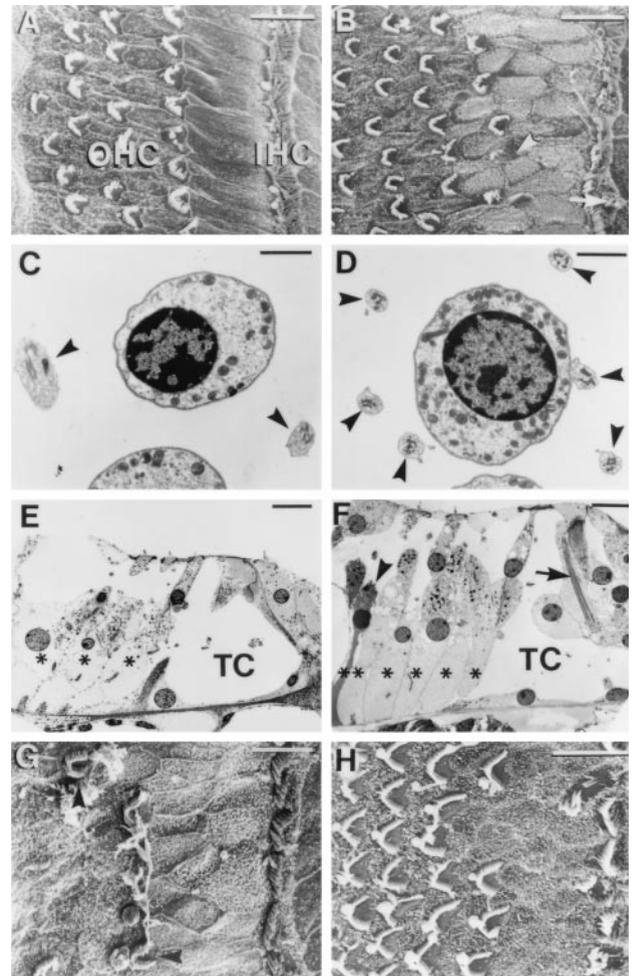


FIG. 3. Morphological comparison of the organ of Corti of adult p27+/+ (wild-type) and p27−/− (homozygote) mice. SEMs of the apical region of p27+/+ (*A*) and p27−/− (*B*) are shown. Note that p27−/− has the fairly typical pattern of three to four rows of OHCs and one row of IHCs as seen in the p27+/+. However, additional (arrow) and abnormal-appearing hair-cells (arrowhead) are seen in p27−/−. Also note that in the region between the IHCs and first row of OHCs in p27−/− there is disorganization of the normal pattern of rectangular apices of the inner pillar cells, with a higher density of irregular apices. (*C*) In p27+/+ at the level of the OHC nuclei, two Deiters'-cell phalangeal processes (arrows) normally can be seen adjacent to a single OHC. (*D*) In the p27−/− mice a single OHC is surrounded by up to six Deiters'-cell phalangeal processes (arrows). (*E*) Radial sections of p27+/+ show normal pillar-cell and phalangeal-cell morphology and number, with three OHC rows and three Deiters'-cell rows (∗), with normal spaces of Nuel and tunnel of Corti (TC). (*F*) In radial sections of p27−/−, there is an increase in the number of Deiters' cells (∗, six) relative to the number of OHC rows (four) present in the section. A Deiters' cell displaying features consistent with apoptotic cell death is also visible (arrowhead). Normal ultrastructural characteristics such as large microtubule bundles can be observed within the pillar cells (arrow), although the cells display distortion that has led to partial collapse of the tunnel of Corti (TC). Also note vesiculation in OHCs. (*G*) SEM of the basal region of the adult p27−/− mouse cochlea showing the presence of a row of IHC stereociliary bundles but a reduced number of OHC bundles. (*H*) SEM of a basal turn in a postnatal day 7 (P7) p27−/− organ of Corti showing a similar supporting-cell phenotype as the adult but up to four rows of OHC bundles. [Bars = 10 $\mu$m (*A*, *B*, *E–H*) and 2 $\mu$m (*C* and *D*).]

to function as a differentiation factor by ectopic expression *in vitro* (26, 27), p27$^{Kip1}$-deficient mice demonstrate true hyperplasia based on increased proliferation. In the multiple organs normally expressing p27$^{Kip1}$, no gross abnormalities or devel-
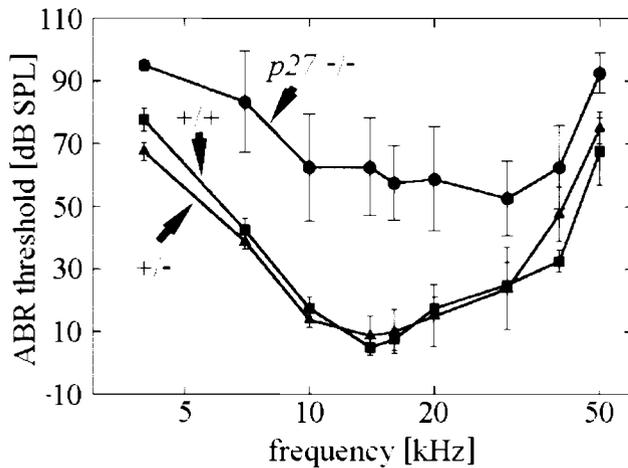
FIG. 4.    ABR thresholds as a function of frequency in the wild-type (p27+/+), heterozygous (p27+/−), and homozygous (p27−/−) mice. Thresholds in both the p27+/+ and the p27+/− are normal but are elevated up to 30 dB at low frequencies (4–7 kHz) and up to 50 dB at higher-frequency regions in p27−/− mice. Threshold elevations are highly significant ($P < 0.0001$) at all frequency points as calculated by repeated-measure ANOVA using the Wolfinger method due to missing values. (Bars = SD.)

opmental defects have been reported. This indicates a limited role for $p27^{Kip1}$ in differentiation *in vivo* (23, 24) and also argues against a primary $p27^{Kip1}$-gene effect on supporting-cell differentiation in the organ of Corti. However, the highly organized cell pattern of the organ of Corti may provide an exceptional challenge for the spatiotemporal formation and preservation of cytoarchitecture. Therefore, loss of proliferation control could result in the observed distortion at the organ-structure level with secondary effects on differentiation at the single-cell level.

The distortion of cytoarchitecture also may contribute to the degeneration and loss of hair cells, in particular, the OHCs in the basal turn of adult mice. Hair-cell loss explains the impairment of function observed at high frequencies. Elevated thresholds in the low-frequency region of the apical turn may be interpreted as a malfunction of the sound-transduction process of the sensory hair cells caused by the altered cellular pattern or by cell damage as indicated by the observed morphological alterations. Furthermore, they may be a result of methodological properties of our electrophysiologic study: in particular, for stimuli with relatively short rise time (here 1 ms) and high sound intensities (>75 dB SPL), the ABR has a significant component from high-frequency-responsive cells.

The most important result of our study is the demonstration of cell proliferation in the organ of Corti of postnatal day 7–11 and adult mice. Terminal mitosis of cells in the mouse organ of Corti normally is completed at embryonic day 14 (11). Thus, in the p27−/− mice proliferation continues at a robust level for at least 2 weeks after it normally ceases and at a reduced level in adulthood. These findings support the proposition that release from inhibition may provide a means by which proliferation-based hair-cell regeneration may be initiated in the organ of Corti. This may also explain why previous attempts to induce cell proliferation in the organ of Corti by damage and/or the addition of exogenous mitogens have not been able to overcome the barriers set up by negative regulators of cell division in the supporting-cell population of the organ of Corti (20–22). Although in general terms it previously was thought impossible to reverse the fate of such terminally differentiated cells, i.e., by inducing them to reenter the cell-division cycle by the application of mitogens, there now is accumulating evidence from several *in vitro* models that functional inactivation of cell-cycle inhibitors, such as the retinoblastoma protein,

allows this to occur (28–30). Further elucidation of these signaling pathways hopefully will indicate how to achieve cell division in particular cell types and refine our ability to induce cell-selective proliferation. It remains to be determined whether release from such inhibition not only will cause cell proliferation in the organ of Corti but also initiate further steps required for hair-cell differentiation, maturation, and functional recovery to complete the hair-cell regeneration process.

1.  Balak, K. J., Corwin, J. T. & Jones, J. E. (1990) *J. Neurosci.* **10,** 2502–2512.
2.  Jones, J. E. & Corwin, J. T. (1996) *J. Neurosci.* **16,** 649–662.
3.  Cotanche, D. A. (1987) *Hear. Res.* **30,** 181–195.
4.  Cruz, R. M., Lambert, P. R. & Rubel, E. W. (1987) *Otol. Head Neck Surg.* **113,** 1058–1062.
5.  Ryals, B. M. & Rubel, E. W. (1988) *Science* **240,** 1774–1776.
6.  Corwin, J. T. & Cotanche, D. A. (1988) *Science* **240,** 1772–1774.
7.  Zheng, J. L., Helbig, C. & Gao, W. Q. (1997) *J. Neurosci.* **17,** 216–226.
8.  Navaratnam, D. S., Su, H. S., Scott, S. P. & Oberholtzer, J. C. (1996) *Nat. Med.* **2,** 1136–1139.
9.  Oesterle, E. C., Tsue, T. T. & Rubel, E. W. (1997) *J. Comp. Neurol.* **380,** 262–274.
10. Katayama, A. & Corwin, J. T. (1989) *J. Comp. Neurol.* **281,** 129–135.
11. Ruben, R. J. (1967) *Acta Otolaryngol. (Stockholm)* **220,** Suppl., 1–44.
12. Corwin, J. T. & Oberholtzer, J. C. (1997) *Neuron* **19,** 951.
13. Chardin, S. & Romand, R. (1995) *Science* **267,** 707–711.
14. Roberson, D. W. & Rubel, E. W (1994) *Am. J. Otology* **15,** 28–34.
15. Sobkowicz, H. M., August, B. K. & Slapnick, S. M. (1997) *Int. J. Dev. Neurosci.* **15,** 463–485.
16. Sidle, A., Palaty, C., Dirks, P., Wiggan, O., Kiess, M., Gill, R. M., Wong, A. K. & Hamel, P. A. (1996) *Crit. Rev. Biochem. Mol. Biol.* **31,** 237–271.
17. Tam, S. K., Gu, W., Mahdavi, V. & Nadal-Ginard, B. (1995) *Ann. N. Y. Acad. Sci.* **752,** 72–79.
18. Ferrari, S., Grande, A., Manfredini, R. & Torelli, U. (1992) *Ann. N. Y. Acad. Sci.* **663,** 180–186.
19. Goldstein, S. (1990) *Science* **249,** 1129–1133.
20. Matsuoka, S., Edwards, M. C., Bai, C., Parker, S., Zhang, P., Baldini, A., Harper, J. W. & Elledge, S. J. (1995) *Genes Dev.* **9,** 639.
21. Parker, S. B., Eichele, G., Zhang, P., Rawls, A., Sands, A. T., Bradley, A., Olson, E. N., Harper, J. W. & Elledge, S. J. (1995) *Science* **267,** 1024–1027.
22. Harper, J. W. & Elledge, S. J. (1996) *Curr. Opin. Gen. Dev.* **6,** 56–64.
23. Fero, M. L., Rivkin, M., Tasch, M., Porter, P., Carow, C. E., Firpo, E., Polyak, K., Tsai, L. H., Broudy, V., Perlmutter, R. M., *et al.* (1996) *Cell* **85,** 733–744.
24. Kiyokawa, H., Kineman, R. D., Manova-Todorova, K. O., Soares, V. C., Hoffman, E. S., Ono, M., Khanam, D., Hayday, A. C., Frohman, L. A. & Koff, A. (1996) *Cell* **85,** 721–732.
25. Nakayama, K., Ishida, N., Shirane, M., Inomata, A., Inoue, T., Shishido, N., Horii, J., Loh, D. Y. & Nakayama, K. (1996) *Cell* **85,** 707–720.
26. Kranenburg, O., Scharnhorst, V., Van der Eb, A. J. & Zantema, A. (1995) *J. Cell. Biol.* **13,** 227–234.
27. Liu, M., Lee, M. H., Cohen, M., Bommakanti, M. & Freedman, L. P. (1996) *Genes Dev.* **10,** 142–153.
28. Schneider, J. W., Gu, W., Zhu, L., Mahdavi, V. & Nadal-Ginard, B. (1994) *Science* **264,** 1467–1471.
29. Kranenburg, O., van der Eb, A. J. & Zantema, A. (1995) *FEBS Lett.* **367,** 103–106.
30. Tiainen, M., Spitkovsky, D., Jansen-Durr, P., Sacchi, A. & Crescenzi, M. (1996) *Mol. Cell. Biol.* **16,** 5302–5312.